Transport properties of high-temperature superconductors: Surface vs bulk effect

L. Burlachkov
Jack and Pearl Resnick Institute for Advanced Technology and Institute of Superconductivity, Department of Physics, Bar-Ilan University, Ramat-Gan 52900, Israel

A. E. Koshelev and V. M. Vinokur
Materials Science Division, Argonne National Laboratory, Argonne, Illinois 60439
(Received 19 December 1995)

We investigate surface-related transport properties of high-temperature superconductors. We find the mean vortex velocity under applied transport current determined by the activation energies for vortex penetration and exit through the Bean-Livingston barrier. We determine the current distribution between the surfaces of superconductor and the field and current dependencies of the transport activation energies. For a three-dimensional superconductor the transport activation energy, U_s^{3D}, is found to decrease with the external field, H, and transport current, J, as $U_s^{3D} \propto H^{-1/2}$ and $U_s^{3D} \propto J^{-1/2}$, respectively. In the quasi-two-dimensional compounds, U_s^{2D} decays logarithmically with field and current. The interplay between the surface and the bulk contributions to the transport properties, such as current-voltage characteristics, is discussed. [S0163-1829(96)00530-9]

I. INTRODUCTION

The properties of the irreversible state of high-temperature superconductors are strongly influenced by the Bean-Livingston surface barrier.[1] This barrier, which affects the vortex entry in (and exit from) a superconductor in external magnetic field H, results from the competition between vortex attraction to the surface (''mirror image'' effect) and its repulsion from the surface due to the Lorentz interaction with the shielding current. In order to enable flux penetration into a superconductor, the shielding current should be strong enough to pull the vortex away from its mirror image over a distance of order of the coherence length, ξ. This condition defines the penetration field, H_p, which exceeds the first critical field, H_{c1}. For a perfect surface one gets[2] $H_p \simeq H_c \simeq \kappa H_{c1}/\ln\kappa$, where H_c is the thermodynamic field and $\kappa = \lambda/\xi$ is the Ginzburg-Landau parameter (λ being the penetration depth). For high-temperature superconductors, such as $YBa_2Cu_3O_{7-x}$ (YBCO) and $Bi_2Sr_2CaCu_2O_8$ (BSCCO) compounds, κ is large ($\kappa \simeq 100$), therefore $H_c/H_{c1} \simeq \kappa/\ln\kappa \simeq 20$, which implies a pronounced surface effect. In real samples the barrier is diminished by surface imperfections, thus H_p lies somewhere in between: $H_{c1} < H_p < H_c$.[3]

The importance of the Bean-Livingston surface barrier in high-temperature superconductors was recognized in Refs. 3–6. The dominant role of the surface barrier in the formation of the magnetization properties of clean untwinned YBCO crystals at high temperatures was demonstrated by Konczykowski *et al.*,[3] who observed the following.

(1) Vanishing of the magnetization ($|M_{\rm exit}| \ll |M_{\rm entry}|$) at the descending branch of the magnetization loop due to the disappearance of surface barrier for flux exit at $H \approx B$, where B is the magnetic induction inside the sample, whereas most bulk pinning (Bean-like) models imply $|M_{\rm entry}| \simeq |M_{\rm exit}|$.

(2) The homogeneous distribution of magnetic induction B inside the sample demonstrated by the Hall probe scanning,[7] which agrees with the surface mechanism of irreversibility and contradicts any bulk pinning model.

(3) Almost complete shrinkage of the magnetization loop $\Delta M = M_{\rm entry} - M_{\rm exit}$ and drastic reduction of H_p as a result of a low-dose ($\simeq 3 \times 10^4$ displacements per atom) electron irradiation,[3] the transition temperature T_c remaining unchanged. This effect of irradiation upon a surface barrier is quite natural since the Frenkel pairs (vacancy + displaced atom) produced by irradiation migrate towards the surface during annealing and form there an amorphous layer, destroying the barrier. On the other hand, one cannot expect reduction of ΔM or H_p due to irradiation for any bulk pinning model, since the latter anyway adds extra defects.

Other evidence for the role of the surface barrier was obtained by the observation of the crossover, which separates the bulk and the surface regimes in the magnetic relaxation rate;[8] analysis of critical fields and irreversibility line $H_{\rm irr}(T)$ in YBCO,[5,9] BSCCO,[10] Tl- (Ref. 11) and Hg-based[12,13] compounds. The influence of the surface barrier on the magnetization properties, flux structure inside a superconductor, and vortex relaxation have been analyzed in Refs. 14–18, where several methods to detect the surface effects and to discriminate between the surface and the bulk contributions to the magnetization were suggested.

In this paper we focus on the effect of the surface barrier on the transport properties, such as transport critical currents J_c and current-voltage characteristics. We find the current (J), field (H), temperature (T), and sample geometry dependencies of the surface activation energies, U_s. These dependencies prove to be quite different from those related to the bulk pinning and could help to distinguish between the surface and bulk contributions to transport characteristics in high-temperature superconductors. This provides better understanding of different regimes of vortex dynamics, such as thermally assisted flux flow (TAFF).

The paper is organized as follows. In Sec. II we briefly review the results on the surface-controlled irreversible mag-

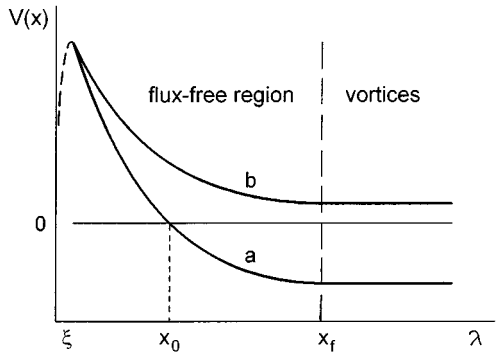

FIG. 1. The potential energy of a straight test vortex near the surface for (a) flux entry; (b) flux exit. At $x>x_f$ the energy $4\pi V(x)/\phi_0=H_{\rm eq}(B)-H\cong m_{\rm eq}-m$. The region $x\sim\xi$, where the ''mirror image'' term $S(x)$ is essential, is shown by a dashed line.

netization. In Sec. III we describe surface activation energies determining flux exit and entry in three-dimensional (3D) and 2D superconductors. Using these results we develop a theory of the surface-related transport in Sec. IV.

II. SURFACE MAGNETIZATION

The energy barrier for a single vortex placed near a superconductor-dielectric boundary was first considered by Bean and Livingston[1] (see also Ref. 2). The barrier for vortex entry disappears at $H=H_p>H_{c1}$, where the shielding current j becomes strong enough to pull a penetrating vortex away from the surface at distances $x\simeq\xi$. The barrier for flux exit disappears at $j=0$ (i.e., on removal of the external field: $H=0$), since the repulsion of a vortex from the surface due to shielding current $j(x)=(cH/4\pi\lambda)\exp(-x/\lambda)$ dominates at $x\geqslant\lambda$ upon the ''short-range'' mirror image interaction $S\propto\exp(-2x/\lambda)$.

In a general case the vortex lattice is already present inside a superconductor, and its interaction between the test vortex, which enters or escapes the sample should be accounted for. This problem was solved by Clem,[14] who considered a continuous flux distribution inside a superconductor, and Ternovskii and Shekhata,[15] who analyzed the stable states of vortex lattice near the surface. The results obtained by both approaches are similar. Both predict the existence of a vortex-free region of the width

$$x_f=\lambda\cosh^{-1}(H/B) \tag{1}$$

near the surface, as shown in Fig. 1. At equilibrium magnetization, where $B=B_{\rm eq}(H)>H-H_{c1}$, one gets $x_f\simeq a$, where $a\simeq(\phi_0/B)^{1/2}$ is the vortex lattice constant, i.e., the vortex-free region shrinks. Within the continuous approximation the potential for a test vortex, shown in Fig. 1, can be written for $0<x<x_f$ as[14]

$$V(x)=\frac{\phi_0}{4\pi}[h(x)-B-H+H_{\rm eq}(B)+S(x)], \tag{2}$$

where

$$h(x)=B\cosh\frac{x_f-x}{\lambda} \tag{3}$$

is the local magnetic field and $S(x)<0$ describes the attraction between the vortex and its mirror image. For a straight infinite vortex $S(x)=S_0(x)=-(\phi_0/4\pi\lambda^2)K_0(2x/\lambda)$ per unit length, where K_0 is the Macdonald function.

For both Abrikosov lines (3D case) and two-dimensional pancakes (2D case) the condition of elimination of the barrier for flux entry at $H>H_p$ is[14,15]

$$m_{\rm en}=H-\sqrt{H^2-H_p^2}\left(\approx\frac{H_p^2}{2H}\ \text{at}\ H\gg H_p\right), \tag{4}$$

where $m\equiv H-B=4\pi M$. For the flux exit[15]

$$m_{\rm ex}=-\frac{\sqrt{3}\phi_0}{48\lambda^2}\approx-\frac{H^*}{2}, \tag{5}$$

where $H^*=\phi_0/4\pi\lambda^2=H_{c1}/\ln\kappa$. Thus $|m_{\rm ex}|\ll H_{c1}\simeq H-B_{\rm eq}(H)\equiv m_{\rm eq}$, where $m_{\rm eq}\simeq(H^*/2)\ln(H_{c2}/B)$ is the equilibrium magnetization. This result generalizes the Bean-Livingston condition $j=0$ for flux escape, which implies $m_{\rm ex}=0$. The ''continuous'' approach[14] provides m_{ex} of the same order of smallness, but of an opposite sign. A recent numerical study[19] of flux dynamics in finite samples on the basis of simulations of the time-dependent Ginzburg-Landau equations confirm Eq. (5). If the bulk pinning is negligible, then the magnetization curve $m(H)$ is due to the surface barrier only, and its ascending and descending branches are determined by Eqs. (4) and (5), respectively. For greater detail see Ref. 17.

Using Eq. (4) and estimating $m_{\rm eq}\simeq(H^*/2)\ln\kappa=H_{c1}/2$ at $H_p\leqslant H\leqslant H_c$,[6] one obtains for $H>H_p$

$$\frac{m_{\rm en}}{m_{\rm eq}}\simeq\frac{H_p^2}{H_{c1}H}\simeq\frac{H_p^2}{H_c^2}\frac{H_{c2}}{H\ln\kappa} \tag{6}$$

For a perfect surface, where $H_p\simeq H_c$, we get from Eq. (6) $m_{\rm en}/m_{\rm eq}\simeq H_{c2}/H\ln\kappa$, i.e., $m_{\rm en}(H)>m_{\rm eq}(H)$ for the whole London regime $H\ll H_{c2}$. But usually the Bean-Livingston barrier is diminished by surface imperfectness:[3,6] $H_{c1}<H_p<H_c$. Then $m_{\rm en}(H)=m_{\rm eq}(H)$ at the surface irreversibility field[18]

$$H^{\rm irr}\simeq H_p^2/H_{c1} \tag{7}$$

which was observed experimentally.[10,11,13]

Due to vortex creep over the barrier, which is especially pronounced for 2D pancakes, the whole magnetization curve described by Eqs. (4) and (5) the effective penetration field H_p proves[4,18] to depend on temperature as

$$H_p=H_{p0}\exp(-T/T_{\rm 2D}),\ \text{2D case}, \tag{8}$$

$$H_p=H_{p0}(T_{3D}/T),\ \text{3D case}, \tag{9}$$

at a given experimental time window.

III. SURFACE ACTIVATION ENERGIES

A. Three-dimensional (3D) case

The activation energies, related to the flux entry ($U_{\rm en}$) at $m_{\rm en}>m>m_{\rm eq}$ and to flux exit ($U_{\rm ex}$) at $m_{\rm eq}>m>m_{\rm ex}$ were found in Ref. 17. A vortex surmounts the barrier by formation of a nucleus (semiloop), which further spreads along the

surface, see Ref. 20. The analogous thermoactivation mechanism has been discussed[21,22] for the creep of vortices trapped by columnar defects.

For superconductors with large κ, where the curve $H_{eq}(B)$ is almost parallel to the line $H=B$ at $H \gg H_{c1}$, we can substitute $H-H_{eq}$ for $m-m_{eq}$ in Eq. (2). Then the potential $V(x)$, see Eq. (2), for a vortex nucleus acquires the form[17]

$$V^{3D}(x)=\frac{\phi_0}{4\pi}\left[\frac{B}{2}\left(\frac{x_f-x}{\lambda}\right)^2+m_{eq}-m+S(x)\right], \quad x<x_f,$$

$$V^{3D}(x)=\frac{\phi_0}{4\pi}(m_{eq}-m), \quad x\geq x_f, \tag{10}$$

where we expanded $h(x)\approx B+B(x_f-x)^2/2\lambda^2$ at $x_f<\lambda$, see Eq. (3). The latter condition holds everywhere in the $m(H)$ diagram, except a small region $H-H_p \ll H_p$. The ''mirror-image'' term $S\simeq H^*\ln(x/x_f)$ for the case of vortex nucleus (semiloop) is much less than the other terms in Eq. (2) except the small region $x\sim\xi$, and thus can be neglected.[17,20,23] Note that this holds for 3D case only and is not valid for pancakes (2D case), which will be discussed further.

The energy of a critical vortex nucleus (semiloop) can be expressed as[16,20]

$$U^{3D}=\frac{2}{\sqrt{\Gamma}}\int_0^{\tilde{x}}\sqrt{V^{3D}(x)\left(\frac{\phi_0 H^*\ln(\tilde{x}/\xi)}{2\pi}-V^{3D}(x)\right)}\,dx, \tag{11}$$

where $\tilde{x}$ is the characteristic size of a nucleus along the x axis and $\Gamma=m_c/m_{ab}$ is the effective mass anisotropy. For flux entry $\tilde{x}=x_0$, see Fig. 1, and for flux exit $\tilde{x}=x_f$. In Refs. 17 and 20 $H_{c1}=H^*\ln(\lambda/\xi)$ was used instead of $H^*\ln(\tilde{x}/\xi)$, which affects only the logarithmic factors and is not of great importance for further analysis. Equation (11) holds provided we neglect the elastic response of the vortex lattice, which is deformed while a test vortex surmounts the barrier. For a more precise description, including the possibility of collective effects, see Refs. 16 and 24.

Using Eqs. (4), (5), and (10), we get

$$\frac{\tilde{x}}{\xi}=\frac{x_0}{\xi}\approx\frac{H_c}{H_p}\sqrt{\frac{m_{en}}{m}}=\kappa m_{eq}\sqrt{\frac{2}{mH}} \quad \text{(flux entry)}, \tag{12}$$

$$\frac{\tilde{x}}{\xi}=\frac{x_f}{\xi}\approx\frac{H_c}{H_p}\frac{\sqrt{m_{en}m}}{m_{eq}}=\kappa\sqrt{\frac{2m}{H}} \quad \text{(flux exit)}. \tag{13}$$

If $m\gg m_{eq}$, then $x_0/x_f=m_{eq}/m\ll 1$, as follows from Eqs. (12) and (13). Therefore the current density for $x<x_0$ can be considered constant and equal to that flowing exactly at the surface: $j_s=(c/4\pi)dh/dx|_{x=0}=c\sqrt{Hm}/(\pi 2\sqrt{2}\lambda)$, see Eqs. (1) and (3). Thus the nucleus has the shape of semiellipse,[22] and its energy is (compare with Refs. 16 and 20)

$$U_{en}^{3D}\approx\frac{\phi_0\lambda(H^*)^2}{32\sqrt{\Gamma Hm}}\left[\ln\left(\kappa m_{eq}\sqrt{\frac{2}{mH}}\right)\right]^2$$

$$\text{at} \quad m_{eq}\ll m\ll H. \tag{14}$$

A general integration of Eq. (11) results in a cumbersome expression which includes elliptical functions. But a very reasonable approximation for all m except $m\cong m_{en}$ can be obtained[17] by neglecting the term $V^{3D}(x)$ in comparison with $\phi_0 H^*\ln(\tilde{x}/\xi)/2\pi$ in Eq. (11). Then, using Eqs. (10)–(13), one obtains the activation energies for flux entry,

$$U_{en}^{3D}\approx\frac{\phi_0\lambda}{2\pi\sqrt{\Gamma H}}\sqrt{H^*\ln\left(\kappa m_{eq}\sqrt{\frac{2}{mH}}\right)}\left[\sqrt{mm_{eq}}+\tfrac{1}{2}(m-m_{eq})\ln\frac{\sqrt{m}-\sqrt{m_{eq}}}{\sqrt{m}+\sqrt{m_{eq}}}\right], \tag{15}$$

and for flux exit,

$$U_{ex}^{3D}\approx\frac{\phi_0\lambda m}{2\pi\sqrt{\Gamma H}}\sqrt{H^*\ln\left(\kappa\sqrt{\frac{2m}{H}}\right)}. \tag{16}$$

Equation (15) for the case $m\gg m_{eq}$ reduces to Eq. (14) up to a numerical factor $3\pi/8\sqrt{2}\approx 0.83$, which justifies the approximation used above.

It is worth noting that U_{en} and U_{ex} do not depend on the ratio H_p/H_c, i.e., on surface damage. This occurs since H_p/H_c is determined[3,6] by the surface imperfections of the scale ξ, whereas the vortex nucleation takes place at larger scales of $\tilde{x}\gg\xi$ for most $m_{ex}<m<m_{en}$. In order to affect Eqs. (14)–(16), the surface damage should extend to the depth of order $x_f\gg\xi$, which is not the case for clean high-temperature samples. Therefore the surface imperfections of the depth ξ, which are responsible for decreasing of H_p down from H_c, have almost no effect on the surface activation energies U_{en} and U_{ex}. The dependence of U_{en} and U_{ex} on m is quite different, which results in the different relaxation rates for vortex entry and exit.[17]

Near the equilibrium ($m\approx m_{eq}$) the critical nuclei for both flux entry and exit have double-kink structure[16] so that $U_{en}^{3D}(m_{eq})=U_{ex}^{3D}(m_{eq})\equiv U_{eq}^{3D}=2U_k$ with

$$U_k\approx\phi_0\lambda m_{eq}^{3/2}/4\pi\sqrt{\Gamma H}. \tag{17}$$

With the logarithmic accuracy Eqs. (15)–(17) coincide with the expressions derived in Ref. 17. Here we assume that the piece of new vortex line created by the nucleus has the same line energy as existing vortices. Strictly speaking, this is valid only in the vortex liquid state. In the crystalline state, penetration of a new vortex creates surface interstitial with extra linear energy. This leads to crossover to the collective penetration and divergency of the barrier as $m\to m_{eq}$.[16]

For $YBa_2Cu_3O_x$ the estimation of U_{eq} gives

$$U_{eq}^{3D}(\tau)/kT_c\simeq\frac{\tau}{\sqrt{H}}\ 6\times 10^4,$$

where $\tau=(T_c-T)/T_c$, the field H is measured in Oe and we used $H\approx B$, $\Gamma=25$, $\lambda=\lambda_0/\sqrt{1-(T/T_c)^4}\approx\lambda_0/2\sqrt{\tau}$ with $\lambda_0=1400$ Å and $\kappa\approx100$. This shows that surface activation energies for 3D superconductors are pronounced even at $T\simeq T_c$ and moderate fields. Therefore the surface irreversibility should dominate over the bulk one at high temperatures,[25] especially at $T>T_{dp}$, where T_{dp} is the bulk depinning temperature,[26] as has been confirmed experimentally.[3]

B. Two-dimensional (2D) case

In strongly layered superconductors the pancake vortices in different layers penetrate through the surface barrier independently from each other. An analytical solution for the activation energy for such penetration can be obtained neglecting lattice response to the penetrating vortex (''rigid lattice'' approximation). Numerical analysis[24] shows that in the equilibrium this approximation is valid at fields $H\leqslant0.01H_{c2}\sim H_c$.

The energy of a pancake vortex $V^{2D}(x)$ is described by Eqs. (2) and (10) but, contrary to the 3D case, the mirror image term $S(x)$ cannot be neglected. This can be understood as follows: In order to find the activation energy U_{en}^{2D} for a pancake, one has to find the maximum of $V^{2D}(x)$ instead of considering the semiloop energy, see Eq. (11). Neglecting $S(x)$, we get the maximum of $V(x)$ at $x=0$ (i.e., at $x\simeq\xi$), see Eqs. (2) and (10), where the mirror image term $S(x)\propto\ln(x_f/x)$ becomes crucially important. Thus we should consider the expansion of Eq. (2) at distance $x\ll x_f$:[18]

$$V^{2D}(x)=U_0\ln\left(\frac{2.94\alpha x}{\xi}\right)-\frac{\phi_0 d j_s x}{c}, \tag{18}$$

where d is the period of the layered structure and $U_0=d(\phi_0/4\pi\lambda)^2$. The first term in Eq. (18) stands for $S(x)$, and the numerical factor $\alpha<1$ describes the decrease of $S(x)$ due to surface damage (as if the pancakes first appear at distance $\xi/2.94\alpha$ apart from the surface). The penetration field H_p is determined from the condition $\max[V^{2D}(x)]<0$ at $B=0$, which gives $H_p=0.76\alpha H_c$. For $H>H_p$ we get

$$U_{en}^{2D}(m)\approx U_0\ln\left(\frac{H_p}{\sqrt{2mH}}\right). \tag{19}$$

We see that U_{en}^{2D} depends on m only logarithmically, unlike the 3D case.

The activation energy for vortex exit, $U_{ex}^{2D}(m_{eq})$, in the equilibrium coincides with $U_{en}^{2D}(m_{eq})\equiv U_{eq}^{2D}$. Out of equilibrium, the energy change to put an extra pancake vortex into the superconductor is given by $-\phi_0 d(m-m_{eq})/4\pi$. Here, as in the case of 3D vortices, we neglect the energy of the elastic deformation in the vortex lattice due to penetration of an extra pancake which is justified far from equilibrium or above the melting temperature of the lattice. Therefore U_{ex}^{2D} can be estimated at $m_{eq}-m\ll m_{eq}$ as

$$U_{ex}^{2D}(m)=U_{en}^{2D}(m)-\frac{\phi_0 d(m_{eq}-m)}{4\pi}$$

$$\approx U_0\left[\ln\left(\frac{H_p}{\sqrt{2mH}}\right)-\frac{m_{eq}-m}{H^*}\right]. \tag{20}$$

At $m\ll m_{eq}$ we get

$$U_{ex}^{2D}(m)\approx\frac{\phi_0 d}{4\pi}m, \tag{21}$$

i.e., $U_{ex}^{2D}\propto m$, similarly to the 3D case. Both U_{en}^{2D} and U_{ex}^{2D} prove to be weakly (logarithmically) field dependent.

For U_{eq}^{2D} one gets an estimation, see Eqs. (19) and (21):

$$U_{eq}^{2D}(\tau)/kT_c\simeq35\tau,$$

where we used $\lambda_0=2000$ Å, $\kappa\approx100$, and $H\simeq H_c$. This is at least one order of magnitude less than U_{eq}^{3D}, even at high fields $H>10^4$ Oe.

The surface activation energies U_{en} and U_{ex} for both 3D and 2D cases should be compared with that related to the bulk pinning, U_b, in order to elucidate which source of irreversibility, the bulk or the surface, governs the flux creep in the sample. For instance, in the magnetization measurements the bulk and the surface relaxations are separated in time,[8] the first being that characterized by the smallest activation energy.[17] At the same time, the transport properties are mostly determined by the largest U.[25]

Note that for both 2D and 3D cases $U\propto\tau=(T_c-T)/T_c$ at $T\to T_c$.

IV. TRANSPORT CRITICAL CURRENT J_c AND SURFACE RESISTIVITY

A transport current J, flowing through a superconducting sample, induces a vortex motion across the sample in a perpendicular direction, thus leading to energy dissipation and, in turn, to the appearance of the normal resistance R. At $J>J_c$ the flux motion is a nonactivation flux flow, i.e., the activation energy $U=0$. At $J<J_c$ the motion is characterized by a finite $U(J)$. Both J_c and U have been extensively studied for different kinds of the bulk pinning, see Ref. 27 as reviews. In this section we derive the critical currents and activation energies related to the surface barrier and discuss their interplay with the bulk pinning for 3D and 2D cases.

Consider a superconducting slab of thickness w $(0<x<w)$, as shown in Fig. 2, in a magnetic field $H>H_p$ parallel to the z axis, where a transport current J flows along y. Let all the relaxation processes be completed, so in the absence of J we have $m=m_{eq}$ and the surface activation energy U_{eq} is determined by Eqs. (17) and (21) (at $m=m_{eq}$) for 3D and 2D superconductors, respectively.

The transport current J results in asymmetry of the external field H at the sides of the slab. In the geometry shown in Fig. 2, the field H_{in} on the left side $(x=0)$, where vortices enter into the slab, becomes larger than H, while at the opposite side $(x=w)$, where vortices exit outside, the field $H_{out}<H$. From the Maxwell equation $dH/dx=4\pi j/c$, where $j(x)$ is the density of the transport current, we get

$$\Delta H\equiv H_{in}-H_{out}=m_{in}-m_{out}=\frac{4\pi}{c}J\equiv\tilde{J}, \tag{22}$$

where $m_{in}=H_{in}-B$, $m_{out}=H_{out}-B$, and $J=\int_0^w j(x)dx$.

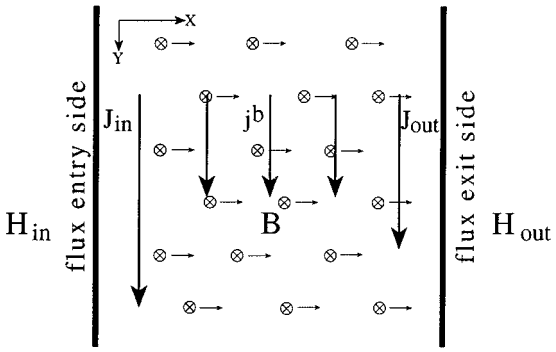

FIG. 2. Distribution of a transport current in superconducting slab. For the case of no bulk pinning $j^b=0$. The arrow corresponding to J_{in} is longer than J_{out} in order to emphasize $J_{in}>J_{out}$ at large currents $\tilde{J}\gg m_{eq}$ for both 3D and 2D cases, see discussion in the text.

The total transport current J flowing in the slab splits into two contributions,

$$J=J^s+J^b, \tag{23}$$

where J^s is the surface contribution and $J^b=j^b w$ is the bulk one (j^b being the current density in the bulk). In turn, J^s consists of two components: $J^s=J_{in}+J_{out}$, see Fig. 2. Obviously,

$$\tilde{J}_{in}=m_{in}-m_{eq}, \tag{24}$$

$$\tilde{J}_{out}=m_{eq}-m_{out}, \tag{25}$$

where $\tilde{J}_{in(out)}=(4\pi/c)J_{in(out)}$.

The magnitudes of J_{in}, J_{out} and J^b are determined by the condition of continuity of flux motion through the slab, which can be written as

$$D_{in}(J_{in})=D_{out}(J_{out})=D_b(j^b)=E/c, \tag{26}$$

where $D_{in}(J_{in})$, $D_{out}(J_{out})$, and $D_b=Bv$ are the flux currents at the surfaces and in the bulk (v being the mean flux velocity in the bulk) and E is the electric field. The average vortex flux through both surfaces is determined by the balance between entry and exit processes shifted by the transport current J. The resulting current-voltage characteristic $J(E)$ can be obtained by solution of Eq. (26) with respect to current components and substitution of the result into Eq. (23).

In strongly nonlinear creep regime the flux currents are determined by the corresponding energy barriers as

$$D_{in}=Bu\omega\ \exp[-U_{en}(m_{eq}+\tilde{J}_{in})/T], \tag{27}$$

$$D_{out}=Bu\omega\ \exp[-U_{ex}(m_{eq}-\tilde{J}_{out})/T], \tag{28}$$

$$D_b=Bu\omega\ \exp[-U_b(j_b)/T], \tag{29}$$

where u and ω are the characteristic hopping distance and frequency, respectively, and $U_{en}(m)$, $U_{ex}(m)$ were derived in Sec. III. Neglecting the difference in the preexponential factors for the surface and the bulk, the redistribution of current is determined by the condition of constant activation energy $U(J)$ at both surfaces and the bulk:

$$U(J)=U_{en}(m_{eq}+\tilde{J}_{in})=U_{ex}(m_{eq}-\tilde{J}_{out})=U_b(j^b). \tag{30}$$

Similarly, the bulk and surface activation energies are equal for the vortex relaxation process, see Ref. 17.

The total critical current J_c at low temperatures, which includes both surface and bulk contribution, is determined by the condition $U_{en}=U_{ex}=U_b=0$, see Eq. (30), which implies $m_{eq}+\tilde{J}_{in}=m_{en}$, $m_{eq}-\tilde{J}_{out}=m_{ex}$, and $j^b=j_c^b$, where j_c^b is the bulk critical current density. Therefore $J_c=J_c^s+J_c^b$, where J_c^s and $J_c^b=j_c^b w$ is the surface and bulk critical currents. For J_c^s, using Eqs. (4) and (5) we get[25]

$$\frac{4\pi}{c}J_c^s\equiv\tilde{J}_c^s=m_{en}-m_{ex}\approx H-\sqrt{H^2-H_p^2}. \tag{31}$$

At $H\gg H_p$, Eq. (31) is reduced to

$$J_c^s\approx\frac{cH_p^2}{8\pi H}, \tag{32}$$

i.e., the surface transport critical current is inversely proportional to the external field H.

At $J\gg J_c^s$ most current flows in the bulk of the sample, and the surface effect on the current-voltage curve is negligible. At $J\leqslant J_c^s$ one has to solve the system of equations (23)–(26), which requires knowledge of the dependence $U_b(j^b)$. However, the general feature of Eqs. (23)–(26) is that for the case of pure surface resistivity (where the bulk pinning is negligible) the activation energy $U=U_s(J)$, and, in turn, the voltage is a function of the *total* transport current J through the sample. For a pure bulk resistivity $U=U_b(j^b)$ is actually a function of the current *density* $j=J/w$. Thus use of samples from the same batch, but of different thickness, can help to determine which kind of pinning, surface or bulk, is dominant. The crossover between bulk and surface transport regimes with changing field, temperature, or current was observed experimentally in thin MoGe films.[28] Below we find functional form of current-voltage curves for 3D and 2D superconductors.

A. 3D case

In the equilibrium vortex liquid state the flux currents $D_{in(out)}$, see Eq. (26), are linear with respect to $J_{in(out)}$ and determined by the surface kinks and antikinks. The surface kink is a piece of vortex line in the flux-free region ending at the surface. At zero transport current the equilibrium concentration of kinks (antikinks) is determined by $n_k=n_{k0}\exp(-U_k/T)$. Extra surface current $J_{in(out)}$ drives kinks and antikinks in opposite directions with velocity $v=\phi_0 J/c\,\eta x_f$ giving rise to net flux currents

$$D_{in(out)}=2\phi_0 n_k v=\frac{2\phi_0 n_{k0}}{c^2\eta x_f}\exp(-U_k/T)J_{in(out)}, \tag{33}$$

where η is the viscosity coefficient of the vortex line directed orthogonally to the surface. This means that small transport current flowing along the sample should be distributed equally between the surfaces, and surface resistivity $R_s=E/(J_{in}+J_{out})$ is given by

$$R_s=\rho_{\rm flow}\frac{Bn_{k0}}{\phi_0 x_f}\exp(-U_k/T), \tag{34}$$

where $\rho_{\rm flow}B\phi_0/c^2\eta$ is the flux-flow resistivity for field orthogonal to the surface. It is important to note that the linear surface resistivity is finite only above the melting temperature of the vortex lattice. If an ordered vortex configuration is present in the bulk, then free surface kinks are topologically forbidden.

The linear regime holds until one can neglect current generation of kinks and antikinks, i.e., until energy of the kink is smaller than the energy of critical nuclei $U_{\rm en}^{\rm 3D}$ and $U_{\rm ex}^{\rm 3D}$. In the opposite limit penetration rates are determined by formation of critical nuclei and given by Eqs. (27) and (28). In order to find the surface activation energy U_s as a function of J^s in this regime, we have to solve Eqs. (30), (22), and (23), using $U_{\rm en}(m)$, $U_{\rm ex}(m)$ derived in Sec. III. After straightforward calculations we get at small surface transport currents $\widetilde{J}^s\ll m_{\rm eq}$:

$$\frac{\widetilde{J}_{\rm in}}{2}\ln\frac{4m_{\rm eq}}{\widetilde{J}_{\rm in}}=\widetilde{J}^s. \tag{35}$$

Under the logarithm in Eq. (35) one can estimate $\widetilde{J}_{\rm in}\simeq\widetilde{J}^s$, thus $\widetilde{J}_{\rm in}\simeq\widetilde{J}^s/\ln(4m_{\rm eq}/\widetilde{J}^s)$ at $\widetilde{J}^s\ll m_{\rm eq}$. As follows from Eq. (35), $\widetilde{J}_{\rm in}/\widetilde{J}^s\to 0$ and $\widetilde{J}_{\rm out}/\widetilde{J}^s\to 1$ at $\widetilde{J}^s\to 0$, which means that in the limit of small currents all the surface transport current flows along the ''flux out'' (vortex exit) side of the sample. Thus

$$U_s^{\rm 3D}(\widetilde{J}^s)=U_{\rm eq}^{\rm 3D}-A\widetilde{J}^s\quad(\widetilde{J}^s\ll m_{\rm eq}),$$

where $A=(\phi_0\lambda/2\pi\sqrt{\Gamma H})\sqrt{H^*\ln(\kappa\sqrt{2m_{\rm eq}/H})}$, see Eqs. (16) and (17).

At $\widetilde{J}^s\gg m_{\rm eq}$ we get

$$\widetilde{J}_{\rm in}\approx\widetilde{J}^s-m_{\rm eq}+\tfrac{2}{3}\sqrt{m_{\rm eq}^3/\widetilde{J}^s},$$

$$m_{\rm in}\approx\widetilde{J}^s[1+\tfrac{2}{3}(m_{\rm eq}/\widetilde{J}^s)^{3/2}]\simeq\widetilde{J}^s, \tag{36}$$

$$\widetilde{J}_{\rm out}\approx m_{\rm eq}-\tfrac{2}{3}\sqrt{m_{\rm eq}^3/\widetilde{J}^s},$$

$$m_{\rm out}\approx\tfrac{2}{3}\sqrt{m_{\rm eq}^3/\widetilde{J}^s}, \tag{37}$$

and

$$U_s^{\rm 3D}(\widetilde{J}^s)\approx Am_{\rm out}\approx\tfrac{2}{3}A\sqrt{m_{\rm eq}^3/\widetilde{J}^s}, \tag{38}$$

see Eq. (16). Contrary to the case of small currents, at $\widetilde{J}^s\gg m_{\rm eq}$ we get $\widetilde{J}_{\rm in}\gg\widetilde{J}_{\rm out}$, i.e., most current flows along the ''flux in'' (vortex entry) side.

The dependencies of $J_{\rm in}$, $J_{\rm out}$, and $U_s^{\rm 3D}$ on J^s, determined by Eqs. (35)–(38) are shown in Fig. 3.

B. 2D case

For 2D superconductor carrying transport current the rates of flux entry and exit can be written as

$$D_{\rm in}=D_0\left[\exp\left(-\frac{U_{\rm en}^{\rm 2D}(m_{\rm eq}+\widetilde{J}_{\rm in})}{T}\right)-\exp\left(-\frac{U_{\rm ex}^{\rm 2D}(m_{\rm eq}+\widetilde{J}_{\rm in})}{T}\right)\right], \tag{39}$$

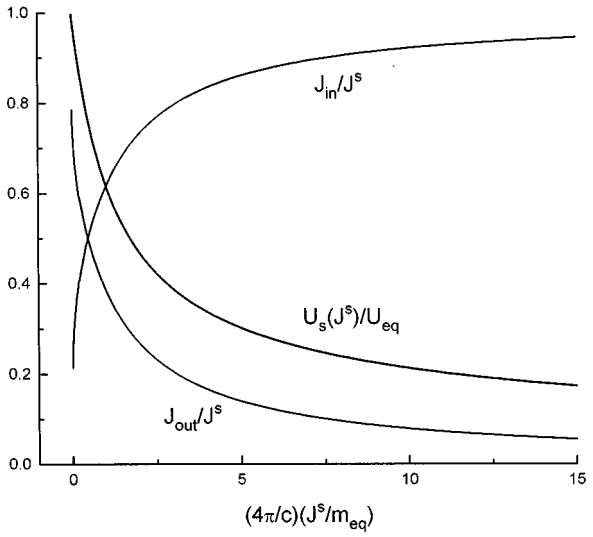

FIG. 3. Dependencies of the current components $J_{\rm in}/J^s$, $J_{\rm out}/J^s$ and the surface activation energy $U_s^{\rm 3D}(J^s)/U_{\rm eq}^{\rm 3D}$ on the surface transport current J^s for the 3D case.

$$D_{\rm out}=-D_0\left[\exp\left(-\frac{U_{\rm en}^{\rm 2D}(m_{\rm eq}-\widetilde{J}_{\rm out})}{T}\right)-\exp\left(-\frac{U_{\rm ex}^{\rm 2D}(m_{\rm eq}-\widetilde{J}_{\rm out})}{T}\right)\right], \tag{40}$$

where $U_{\rm en}^{\rm 2D}(m)$ and $U_{\rm ex}^{\rm 2D}(m)$ are the barriers for flux entry and flux exit given by Eqs. (19) and (20). Here, unlike the 3D case, we took into account the ''backward'' jumps of pancakes from lower potential to the higher one (against the Lorentz force). The backward processes are restricted for 3D vortex lines, where a vortex surmounts the barrier by formation a nucleus, since such a nucleus cannot be formed if $V(x)>0$ at all x, see Sec. III. For 2D pancakes, which enter and exit the sample separately, the backward jumps can be essential. As for the 3D case in steady state

$$D_{\rm in}(\widetilde{J}_{\rm in})=D_{\rm out}(\widetilde{J}_{\rm out})=E/c. \tag{41}$$

These conditions determine the redistribution of current between surfaces and determine the current-voltage curves. One can distinguish several current regimes. At very small transport current, $\widetilde{J}^s\ll T/\phi_0 d$, it distributes equally between the surfaces and the surface resistivity $R_s=E/(J_{\rm in}+J_{\rm out})$ is linear and given by

$$R_s=\frac{\phi_0 dD_0}{2T}\exp\left(-\frac{U_{\rm eq}^{\rm 2D}}{T}\right). \tag{42}$$

The surface dominates in the linear transport for narrow enough sample or/and at low enough temperatures:

$$w<\rho_b/R_s=\frac{2T\rho_b}{\phi_0 dD_0}\exp\left(\frac{U_{\rm eq}^{\rm 2D}}{T}\right), \tag{43}$$

where w is the width of the sample and ρ_b is the bulk linear resistivity.

At $\tilde{J}^s \gg T/\phi_0 d$ the backward jumps can be neglected and we obtain

$$D_{\rm in} \approx D_0 \exp\left(-\frac{U_{\rm en}^{\rm 2D}(m_{\rm eq}+\tilde{J}_{\rm in})}{T}\right),$$

$$D_{\rm out} \approx D_0 \exp\left(-\frac{U_{\rm ex}^{\rm 2D}(m_{\rm eq}-\tilde{J}_{\rm out})}{T}\right), \qquad (44)$$

and surface resistivity becomes strongly nonlinear. Using Eqs. (19), (20), and (41), the distribution of the moderate, but not very weak, current $T/\phi_0 d \ll \tilde{J}^s \ll m_{\rm eq}$ between the flux entry and flux exit sides of the sample can be estimated as

$$\tilde{J}_{\rm in} \approx \frac{H_c H^*}{2B}\left(\frac{E}{cD_0}\right)^{2T/U_0} - m_{\rm eq}, \qquad (45)$$

$$\tilde{J}_{\rm out} \approx m_{\rm eq} - \frac{4\pi T}{\phi_0 d}\ln\frac{cD_0}{E} - \frac{H^*}{2}\ln\left[\ln\frac{m_{\rm eq}}{H^*} + \frac{2T}{U_0}\ln\frac{cD_0}{E}\right], \qquad (46)$$

where J_c^s is the surface critical current given by Eq. (32).

For large currents $\tilde{J}^s \gg m_{\rm eq}$ one finds

$$\tilde{J}_{\rm in} \approx \tilde{J}^s - m_{\rm eq} + H^* \ln(H_p/\sqrt{2\tilde{J}^s H}), \qquad (47)$$

$$\tilde{J}_{\rm out} \approx m_{\rm eq} - H^* \ln(H_p/\sqrt{2\tilde{J}^s H}) \ll \tilde{J}_{\rm in}, \qquad (48)$$

and

$$U_s^{\rm 2D}(\tilde{J}^s) \approx U_0 \ln(H_p/\sqrt{2\tilde{J}^s H}).$$

As for 3D superconductors, in the limit of large currents $\tilde{J}^s \gg m_{\rm eq}$ most transport current flows along the ''flux entry'' side of the slab.

Complete current-voltage curve in the nonlinear regime can be written as

$$J(E) = \frac{Ew}{\rho_b} + 0.6 J_c^s\left(\frac{E}{cD_0}\right)^{2T/U_0} - \frac{cT}{\phi_0 d}\ln\frac{cD_0}{E} - \frac{cH^*}{8\pi}\ln\left[\ln\frac{m_{\rm eq}}{H^*} + \frac{2T}{U_0}\ln\frac{cD_0}{E}\right] \quad \text{at} \quad \tilde{J}^s < m_{\rm eq} \qquad (49)$$

and

$$J(E) = \frac{Ew}{\rho_b} + 0.6 J_c^s\left(\frac{E}{cD_0}\right)^{2T/U_0} \quad \text{at} \quad \tilde{J}^s > m_{\rm eq}. \qquad (50)$$

With increase of transport current a larger fraction of current goes to the bulk: $J^b/J \to 1$. When the electric field exceeds the typical value $\rho_b J_c^s/w$, the surface effect on vortex transport becomes weak. This type of behavior was indeed observed experimentally.[28]

V. CONCLUSIONS

We considered the contribution of the surface (Bean-Livingston) barriers to critical transport currents and activation energies in high-temperature superconductors. For both 3D (e.g., YBCO) and 2D (e.g., BSCCO) compounds the surface transport critical current $J_c^s \propto 1/H$ at $H > H_p$. This current should be added to the bulk critical current J_c^b in order to find the total J_c. The surface activation energies $U_s^{\rm 3D}$ and $U_s^{\rm 2D}$ prove to be quite different. The characteristic dependencies of $U_s^{\rm 3D}$ on current and external field are $U_s^{\rm 3D} \propto 1/\sqrt{JH}$, whereas $U_s^{\rm 2D}$ shows a much weaker (logarithmic) dependence: $U_s^{\rm 2D} \propto \ln(H_p\sqrt{4\pi/cJH})$. A weak transport current J, which induces the fields less than $m_{\rm eq} \sim H_{c1}$, can be distributed between the flux entry and exit sides differently depending on dimensionality (2D or 3D) and weakness of J, whereas a large current (with self-fields greater than $m_{\rm eq}$) flows mainly along the ''flux entry side'' for both 3D and 2D superconductors, provided $m_{\rm en} \gg m_{\rm eq}$.

ACKNOWLEDGMENTS

This work was supported by the Israel Academy of Sciences (Project No. 519/94), the Heinrich Hertz Minerva Center for High-Temperature Superconductivity, the U.S. National Science Foundation Office of the Science and Technology Center under Contract No. DMR-91-20000 and by the U.S. Department of Energy, BES-Materials Sciences, under Contract No. W-31-109-ENG-38. V.M.V. acknowledges support from the Rich Foundation (via the Ministry of Science and the Arts of Israel) during visits to Israel.

[1] C.P. Bean and J.D. Livingston, Phys. Rev. Lett. **12**, 14 (1964).
[2] P.G. de Gennes, *Superconductivity of Metals and Alloys* (W.A. Benjamin, Inc., New York, 1966).
[3] M. Konczykowski, L. Burlachkov, Y. Yeshurun, and F. Holtzberg, Phys. Rev. B **43**, 13 707 (1991).
[4] V.N. Kopylov, A.E. Koshelev, I.F. Schegolev, and T.G. Togonidze, Physica C **170**, 291 (1990).
[5] M.W. McElfresh, Y. Yeshurun, A.P. Malozemoff, and F. Holtzberg, Physica A **168**, 308 (1990).
[6] L. Burlachkov, M. Konczykowski, Y. Yeshurun, and F. Holtzberg, J. Appl. Phys. **70**, 5759 (1991).
[7] M. Konczykowski, F. Holtzberg, and P. Lejay, Supercond. Sci. Technol. **4**, 8331 (1991).
[8] N. Chikumoto, M. Konczykowski, N. Motohira, and A.P. Malozemoff, Phys. Rev. Lett. **69**, 1260 (1992).
[9] L. Burlachkov, Y. Yeshurun, M. Konczykowski, and F. Holtzberg, Phys. Rev. B **45**, 8193 (1992).
[10] D. Majer, E. Zeldov, M. Konczykowski, V.B. Geshkenbein, A.I. Larkin, L. Burlachkov, V.M. Vinokur, and N. Chikumoto, Physica C **235-240**, 2765 (1994).
[11] F. Zuo, D. Vacaru, H.M. Duan, and A.M. Hermann, Phys. Rev. B **47**, 5535 (1993).
[12] J.A. Lewis, V.M. Vinokur, J. Wagner, and D. Hinks, Phys. Rev. B **52**, R3852 (1995).
[13] Yang Ren Sun, J.R. Thompson, H.R. Kerchner, D.K. Christen, M. Paranthaman, and J. Brynestad, Phys. Rev. B **50**, 3330 (1994);

Yang Ren Sun, J.R. Thompson, J. Schwartz, D.K. Christen, Y.C. Kim, and M. Paranthaman, *ibid.* **51**, 581 (1995).

[14] J.R. Clem, in *Proceedings of Low Temperature Physics-LT 13*, edited by K.D. Timmerhaus, W.J. O'Sullivan, and E.F. Hammel (Plenum, New York, 1974), Vol. 3, p. 102.

[15] F.F. Ternovskii and L.N. Shekhata, Sov. Phys. JETP **35**, 1202 (1972).

[16] A.E. Koshelev, Physica C **191**, 219 (1992).

[17] L. Burlachkov, Phys. Rev. B **47**, 8056 (1993).

[18] L. Burlachkov, V.B. Geshkenbein, A.E. Koshelev, A.I. Larkin, and V.M. Vinokur, Phys. Rev. B **50**, 16 770 (1994).

[19] D.W. Braun, G.W. Crabtree, H.G. Kaper, A.E. Koshelev, G.K. Leaf, D.M. Levine, and V.M. Vinokur, Phys. Rev. Lett. **76**, 831 (1996).

[20] B.V. Petukhov and V.R. Chechetkin, Sov. Phys. JETP **38**, 827 (1974).

[21] D.R. Nelson and V.M. Vinokur, Phys. Rev. Lett. **68**, 2398 (1992); Phys. Rev. B **48**, 13 060 (1993).

[22] E.H. Brandt, Phys. Rev. Lett. **69**, 1105 (1992).

[23] V.P. Galaiko, Sov. Phys. JETP **23**, 1202 (1966).

[24] A.E. Koshelev, Physica C **223**, 276 (1994).

[25] L. Burlachkov and V.M. Vinokur, Physica B **194-196**, 1819 (1994).

[26] G. Blatter, M.V. Feigel'man, V.B. Geshkenbein, A.I. Larkin, and V.M. Vinokur, Rev. Mod. Phys. **66**, 1125 (1994) .

[27] S. Senoussi, J. Phys. (France) III **2**, 1041 (1992); E.H. Brandt, Rep. Prog. Phys. **58**, 1465 (1995).

[28] W.R. White, A. Kapitulnik, and M.R. Beasley, Phys. Rev. Lett. **70**, 670 (1993).